The Moving Puncture Breakthrough

Diandian Wang

29 April 2017

Abstract

In this report, the developments in Numerical Relativity before and after the moving puncture breakthrough are reviewed. The moving puncture method is based on previous theories including the 3+1 formalism, the ADM equations, and the BSSN formulation. Its main application is in the field of gravitational wave astronomy, where the numerical predictions of the waveforms are used to identify the detected gravitational waves.

1 Introduction

In General Relativity (GR), most of the astrophysical systems of interest do not possess the necessary symmetries for analytic solutions to exist. Perturbation theory is one alternative approach, but as the name suggests, it only works if the system is marginally different from a system with a known solution. Another possibility is to use numerical methods, which might be the only valid approach in more general situations. The importance of Numerical Relativity (NR) is seen in the study of the merger of two black holes (BHs), or binary black hole (BBH) coalescence. Such events were believed to be sources of extremely energetic gravitational waves, which experiments such as LIGO were hoping to detect. However, unlike the Newtonian two-body problem where an analytic solution exists, in GR, the two-body problem is not straightforward. Firstly, because of gravitational wave (GW) emission, the energy of the system dissipates. Secondly, there are no point masses in GR, and the elementary objects are BHs which necessitates the consideration of tidal effects, singularities, etc. Finally, the simple Newtonian equation of motion is replaced by the Einstein Field Equations (EFEs) - a set of coupled, non-linear partial differential equations (PDEs).

The breakthrough came in 2005, when the successful simulation of the merger was finally carried out using two methods: Pretorius' generalised harmonic formulation and the so-called moving puncture technique used by the Goddard and Brownsville groups. The waveform extracted from the simulation of the merger was a key factor that contributed to the identification of the detected gravitational waves announced on 11 February, 2016, which was a triumph in the verification of Einstein's theory of General Relativity formulated a century ago.

In Section 2, we will introduce the 3+1 space-time split of the EFEs, namely the Arnowitt-Deser-Misner (ADM) equations and the Baumgarte-Shapiro-Shibata-Nakamura (BSSN) formalism. In Section 3, we will discuss how to represent and evolve BHs on computers, focusing on the moving puncture approach. Section 4 gives a brief overview of GWs and their relevance to NR. Finally a brief summary will be given in Section 5.

2 The 3+1 formalism

The biggest task of NR is to solve the EFEs,

$$G_{\alpha\beta} + \Lambda g_{\alpha\beta} \equiv R_{\alpha\beta} - \frac{1}{2} g_{\alpha\beta} R + \Lambda g_{\alpha\beta} = \frac{8\pi G}{c^4} T_{\alpha\beta}, \tag{1}$$

where $g_{\alpha\beta}$ is the metric of the four-dimensional manifold, R is the Ricci scalar, $R_{\alpha\beta} = R^{\mu}{}_{\alpha\mu\beta}$ is the Ricci tensor, $T_{\mu\nu}$ is the energy-momentum tensor, $G_{\alpha\beta}$ is the Einstein tensor defined by the equivalence sign, G is the gravitational constant, and c is the speed of light. For simplicity, for the rest of the article, we will employ the geometrised units $G = c = 1$, and adopt the convention '$- + + +$' as the signature for the metric tensor. We also restrict ourselves to the case of vacuum and asymptotically flat spacetimes, i.e., $\Lambda = 0$ and $T_{\alpha\beta} = 0$, so the EFEs become $G_{\alpha\beta} = 0$. For convenience, we let the Greek indices run over spacetime values (0 to 3), while the Latin indices only run over the spatial values (1 to 3).

This set of rather innocent-looking equations is in fact quite involved. The Ricci tensor is a non-linear function of $g_{\alpha\beta}$ and its first and second derivatives. Moreover, in this form, space and time are on equal footing (except for the opposite sign in the metric tensor). This covariant form comes naturally from differential geometry when we consider space and time under a single structure which we call spacetime. In practice however, it is useful to view the evolution of a system in time given an initial spatial setup. For example, we are interested in how the gravitational field evolves in time given the initial states (positions, velocities, spins, etc.) of two nearby BHs. This space-time split is known as the 3+1 formalism, and it allows us to cast our problem as a Cauchy problem.

2.1 The ADM equations

The 3+1 formalism was first formulated in the period from 1920's to 1950's, by Darmois [1], Lichnerowicz [2–4] and Choquet-Bruhat [5, 6]. Then in the late 1950's and early 1960's, Dirac [7, 8], and Arnowitt, Deser and Misner (ADM) [9] readdressed this problem with a Hamiltonian approach in an attempt to quantise gravity. ADM's paper became the most frequently cited work in this aspect, and the canonical 3+1 equations are usually referred to as the ADM equations [10]. The ADM equations were later reformulated by York Jr. [11, 12].

The derivation of the ADM equations requires introducing a few concepts (see e.g. [13] for a more detailed derication). Consider a globally hyperbolic manifold $\mathcal{M}$ with a Lorentzian metric $g_{\alpha\beta}$. It can be shown that any globally hyperbolic spacetime can be completely *foliated* (i.e. sliced into three-dimensional pieces) so that the sliced hypersurfaces are spacelike (see e.g. [14]). The hypersurfaces can be identified with the level sets of a parameter t which we call *universal time function* (but not necessarily the proper time of any observer). We denote the hypersurfaces by Σ_t and call the set of spacelike hypersurfaces a *foliation*. We now choose coordinates *adapted* to the foliation such that $x^0 = t$, and x^i are the spatial coordinates in each hypersurface. Now we define the future-pointing normal $\boldsymbol{n}$, the lapse function α and the shift function $\boldsymbol{\beta}$ as $\boldsymbol{n} \equiv -\frac{\mathbf{d}t}{\|\mathbf{d}t\|}, \alpha \equiv \frac{1}{\|\mathbf{d}t\|}$, and $\boldsymbol{\beta} \equiv (\boldsymbol{\partial}_t) - \alpha\boldsymbol{n}$. One notices that the shift operator $\boldsymbol{\beta}$ is tangent to Σ_t since $\langle \mathbf{d}t, \alpha\boldsymbol{n}\rangle = 1$ and $\langle \mathbf{d}t, \boldsymbol{\partial}_t\rangle = 1$. Also, for an observer with 4-velocity $\boldsymbol{n}$ and proper time τ, we have $\Delta\tau = \alpha\Delta t$, which follows from the definition of $\boldsymbol{n}$ and α (c.f. Figure 1). At this point, we note that both the lapse and the shift can be chosen freely.

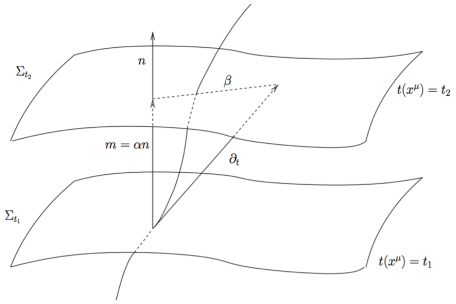

Figure 1: Two hypersurfaces of a foliation with lapse α and shift vector $\boldsymbol{\beta}$ shown. Figure taken from [15].

To be able to cast the problem as a temporally evolving space (spacelike hypersurface), it is useful to define the projection operator $\perp^\alpha{}_\mu \equiv \delta^\alpha{}_\mu + n^\alpha n_\mu$ so that the projection of an arbitrary tensor $T^{\mu_1\mu_2\cdots}{}_{\nu_1\nu_2\ldots}$ is given by

$$(\perp T)^{\alpha_1\alpha_2\cdots}{}_{\beta_1\beta_2\ldots} \equiv \perp^{\alpha_1}{}_{\mu_1} \perp^{\alpha_2}{}_{\mu_2} \ldots \perp^{\nu_1}{}_{\beta_1} \perp^{\nu_2}{}_{\beta_2} \ldots T^{\mu_1\mu_2\cdots}{}_{\nu_1\nu_2\ldots}. \tag{2}$$

In particular, the *spatial metric* (also called the *first fundamental form*) is the projection of the metric to the hypersurface Σ_t,

$$\gamma_{\alpha\beta} \equiv \perp^\mu{}_\alpha \perp^\nu{}_\beta g_{\mu\nu} = g_{\alpha\beta} + n_\alpha n_\beta = \ \perp_{\alpha\beta} . \tag{3}$$

With these definitions, the metric tensor in the adapted coordinate system can be expressed in terms of α, β_j and γ_{ij}, which defines a unique torsion-free and metric compatible connection $\Gamma^i{}_{jk}$, and an associated covariant derivative D_γ for an arbitrary spatial tensor. Next, we define the *extrinsic curvature* $K_{\alpha\beta} \equiv - \perp \nabla_\beta n_\alpha$. As is obvious from the definition, it measures the variation of the normal vector across the hypersurface.

Moreover, for notational convenience, we denote the projections of the energy momentum tensor by the following

$$\rho = T_{\mu\nu} n^\mu n^\nu, \qquad j_\alpha = -\perp^\nu{}_\alpha T_{\mu\nu} n^\mu, \qquad S_{\alpha\beta} = \perp^\mu{}_\alpha \perp^\nu{}_\beta T_{\mu\nu}, \qquad S = \gamma^{\mu\nu} S_{\mu\nu}. \tag{4}$$

Finally, with these definitions at hand, we can rewrite the EFEs in the space-time split form by substituting the three-quantities we have defined above. We obtain the *ADM equations*:

$$\partial_t \gamma_{ij} = \beta^m \partial_m \gamma_{ij} + \gamma_{mj} \partial_i \beta^m + \gamma_{im} \partial_j \beta^m - 2\alpha K_{ij}, \tag{5}$$

$$\begin{aligned} \partial_t K_{ij} = {} & \beta^m \partial_m K_{ij} + K_{mj} \partial_i \beta^m + K_{im} \partial_j \beta^m - D_i D_j \alpha \\ & + \alpha(\mathcal{R}_{ij} + K K_{ij} - 2 K_{im} K^m{}_j) + 4\pi\alpha[(S - \rho)\gamma_{ij} - 2 S_{ij}], \end{aligned} \tag{6}$$

$$0 = \mathcal{R} + K^2 - K^{mn} K_{mn} - 16\pi\rho, \tag{7}$$

$$0 = D_i K - D_m K^m{}_i + 8\pi j_i, \tag{8}$$

where $\mathcal{R}_{ij}$ and $\mathcal{R}$ are the Ricci tensor and scalar corresponding to the three-metric.

2.2 The BSSN formulation

As Nakamura et al. [16] pointed out in 1987, the ADM evolution equations are not stable under long-term numerical simulations, because they are not *well-posed* (a system of PDEs is well-posed if we can define a norm $\|\cdot\|$ such that $\|u(t,x)\| \leq ke^{\alpha t}\|u(0,x)\|$, with k and α being constants independent of the initial data, and u being some n-dimensional vector-valued function of time t and space x).

Nevertheless, all is not lost. The ADM equations are not unique (for example, we can add an arbitrary multiple of the constraint equations to the evolution equations without changing the physical solutions), but doing so could change the mathematical properties of the system. By doing this, the ADM equations can be rewritten in a well-posed form without changing the physics. Several approaches have been formulated to achieve that, such as the Kidder, Scheel, and Teukolsky (KST) formulation [17] which used more than 30 evolution equations and 12 free parameters. Another method is the Baumgarte-Shapiro-Shibata-Nakamura (BSSN) formalism, which became widely used.

BSSN is a modified version of ADM [18]. It originates from the paper by Nakamura et al. [16] in 1987, and the idea was further developed by Shibata et al. [19, 20] and Baumgarte, Shapiro and Yo [21–23] in the following decade. This formulation is empirically driven, but some analytic justification was later provided by Alcubierre et al. [24]. The development of the BSSN method began with the observation that the error growth could be best suppressed if γ, the determinant of γ_{ij}, and K, the trace of K_{ij}, were evolved independently. Several auxiliary variables were introduced to maintain the stability of the numerical simulation (see e.g. [24] for details of the auxiliary variables).

The BSSN formulation has been successful at simulating long-term linear GWs [20, 21], nonlinear GWs [21, 24], rotating black holes [22, 23, 25], etc. Moreover, it was used by the Brownsville [26] and the Goddard [27] groups in the moving puncture scheme for the successful simulation of merging binary black holes in 2005.

3 The moving puncture

Black holes contain spacetime singularities, and representing singularities on a computer is not a trivial task. Two mainstream methods have been used: the excision method first proposed by Unruh [28] and the puncture method. As suggested by the name, the excision method involves cutting the black holes from the computational grid. We will not elaborate on this.

The puncture method exploits the interesting topology of GR around a black hole. Modifying the solution of a spherically symmetric space in an unessential way, Einstein and Rosen [29] were able to show that regular solutions (i.e. solutions with no singularity) exist if the physical space is treated as consisting of two identical 'worldsheets'. Thus, a black hole can be considered as a 'bridge' connecting two worldsheets (see Figure 2), and the 'bridge' is called a *wormhole*. To be more specific, consider a Schwarzschild geometry with the interior of the event horizon removed. We then create an identical copy of this space and superimpose them such that their event horizons coincide. We now require that the two event horizons are in fact the same one; then the resulting geometry is a wormhole geometry. We distinguish the two 'identical' copies by

inserting an asymmetrical coordinate system. A convenient coordinate system was discovered by Brill and Lindquist [30] in 1963 in which the three-metric is

$$\gamma_{ij} = \left(1 + \frac{M}{2R}\right)^4 \delta_{ij}, \tag{9}$$

where R is a radial coordinate, and M is the mass of the black hole. To create an asymmetrical coordinate system, Brill and Lindquist noted that this three-metric is invariant under the transformation $r' = M^2/4R$, and $r' = R$ when $R = m/2$. With this, we can create a global coordinate variable r' covering both worldsheets (the worldsheets being denoted by A and B), by transforming their radial coordinates, R_A and R_B by:

$$R_A = r' \text{ for } r' \geq \frac{M}{2}, \qquad R_B = \frac{M^2}{2r'} \text{ for } r' \leq \frac{M}{2}. \tag{10}$$

If we label the physical world we are (interested) in by A, then the coordinate $r' = \infty$ is at the spatial infinity of the physical world, while $r' = 0$ is at the spatial infinity of the mirror world (see Figure 2). Thus, we have evaded the physical singularity, but at the cost of a coordinate singularity at $r' = 0$ which we call a 'puncture'. Fortunately, the coordinate singularity can be restricted to a single scalar field, and this irregular field can be handled numerically [31].

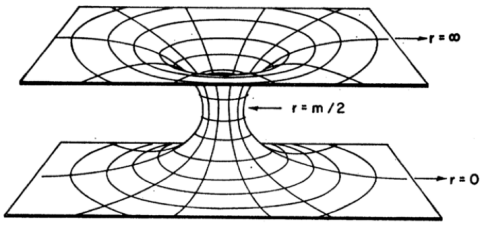

Figure 2: A wormhole joining a two-dimensional space (the upper sheet) and its duplicate (the lower sheet). In the Brill-Lindquist coordinate, the coordinate singularity, $r = 0$, is at the spatial infinity of the duplicate. Figure taken from [30].

Originally, gauge conditions were chosen to make the punctures remain at fixed coordinate positions. However, in the simulation of inspiralling black holes, for example, the physical distance decreases with time and the steep gradients undergo substantial dynamics. Moreover, as the black holes orbit around each other, there is some twisting of the coordinates [31]. Both features cause numerical instabilities, so having the punctures fixed did not lead to any success.

The breakthrough came in 2005, when Baker et al. at the NASA Goddard Space Flight Center [27] and Campanelli et al. at the University of Texas at Brownsville [26] independently discovered that, with some modifications of the gauge conditions used for the fixed punctures, the punctures can be moved arbitrarily and the resulting numerics was stable. This finally permitted accurate and long-term evolution of BBH systems. This upgraded version of the 'fixed puncture method' with punctures now in motion is referred to as the 'moving puncture method'.

4 Gravitational waves

The coalescence of BBH can be divided into three stages: inspiral, merger and ringdown. In the inspiral stage, two black holes rotate around each other, and as time elapses, they progress towards each other. In the merger stage, the black holes start to combine (their horizons join) and form a distorted black hole. In the ringdown stage, the distorted black hole stabilises to a quiescent black hole after emission of GWs [32]. Probably the most important application of the BBH simulation is to provide the predicted waveforms for an observer at infinity. As the computational grid has to be finite, the waveform at infinity must be found by extrapolation (see [33] for a description of an extrapolation method).

4.1 Propagation of GWs in empty space

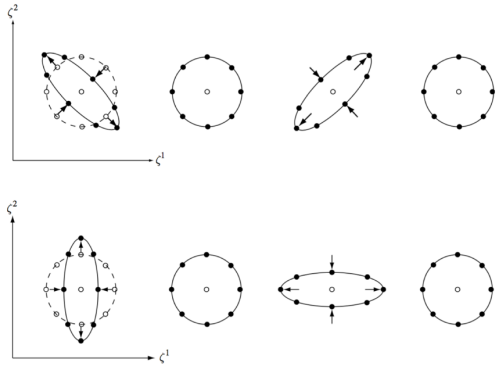

Figure 3: Two polarisations of plane GWs viewed along the z-axis. The dots represent the positions of a set of circularly arranged point masses under the influence of the wave. Each configuration has a $\pi/2$ phase difference to the previous one. Figure taken from [34].

In GR, the EFEs play the role of the Maxwell equations in Electromagnetism, and in an analogous manner, analytic propagating wave solutions exist in the weak field limit. Unlike electromagnetic radiations which can have a dipole character, conservation of linear and angular momentum means the leading order contribution to GWs is quadrupolar [35]. In practice, waves of interest are generated in strong-field regions, where numerics is needed. We can however study the form of the wave analytically in the weak field regime corresponding to when the wave has propagated far enough from the source.

A *weak* gravitational field refers a region of space that is 'almost flat'. More precisely, the metric in such a region takes the form $g_{\mu\nu} = \eta_{\mu\nu} + h_{\mu\nu}$, with $|h_{\mu\nu}| = \mathcal{O}(\epsilon) \ll 1$, where $\eta_{\mu\nu}$ is the Minkowski metric, and $\epsilon \ll 1$ is a small parameter. In this limit, a linearised theory can be developed by expanding all terms in the EFEs in powers of ϵ and keeping only linear order terms. It can be shown that there exist solutions of the form $h^{\mu\nu} = A^{\mu\nu} \exp(ik_\rho x^\rho)$, where $A^{\mu\nu}$ are constants and have only two independent components due to freedom in coordinate transformation. The two degrees of freedom correspond to two polarisations of the wave (see Figure 3), and any general plane wave can be represented as a linear combination of the two.

4.2 Numerical results and detection of GWs

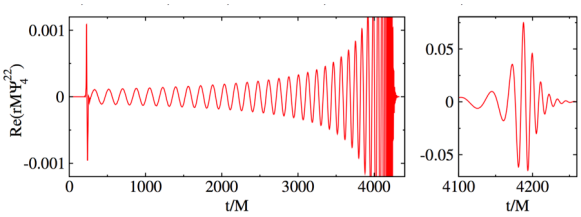

Figure 4: Gravitational waveform extraction at $r = 225M$ obtained by Scheel et al. [36]. The left subfigure shows the overall waveform, while the right subfigure focuses on the merger and the ringdown stages. The pulse at around $t = 200M$ is the 'junk radiation' (caused by imperfect initial data not being exactly in equilibrium).

Following the breakthroughs in 2005, many more BBH simulations have been carried out. Figure 4 shows a typical waveform extracted at a distant point obtained by Scheel et al. [36] in 2009. The overall form of radiation, especially that of the last two stages, is a signature of the BBH coalescence. Looking for this signature is the key in wave-detection stations such as LIGO, Virgo and LISA.

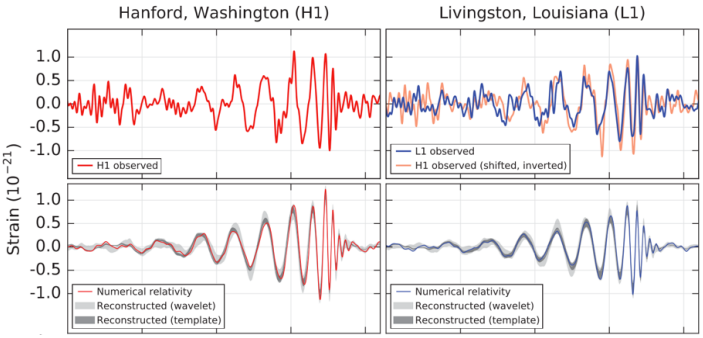

Figure 5: GW signals observed by LIGO Hanford (left column panels) and Livingston (right column panels) detectors. Figure taken from [37].

The expected waveform was finally detected by LIGO on 14 September, 2015 and announced on 11 February, 2016 (see Figure 5). This monumental event, which occurred a century after Einstein published the paper on GR, gave the first direct test of the strong-field regime of the theory, and at the same time demonstrated the importance of NR.

4.3 Further remarks

Although other compact binary mergers (i.e. a BH and a neutron star or double neutron stars) are much weaker sources of GW, it is highly likely that signals emitted by them will be detected in the near future. Soon after the first GW detection, Belczynski et al. [38] showed that an increase of $\sim$2.5 in the instrument sensitivity should allow the detection of GW emitted from them. Currently, the instrument at LIGO/Virgo is being upgraded and is expected to reach its target sensitivity in 2019, which is more than 2.5 times the current sensitivity [38].

The direct detection of GWs has undoubtedly started a new era in observational astronomy. However, the astronomical environment (e.g. medium density) of the BBH cannot be determined solely from the GW signals as a result of the large sky localisation uncertainties (∼600 square degrees for the first event) [37, 39]. Thus, electromagnetic signals are also needed. For example, for neutron star merging with a BH, as a result of large tidal torques, energy and angular momentum are removed on a small time scale, after which the decompression could lead to synthesis of radioactive elements through the r-process [40, 41]; its radioactive decay could then give rise to an optical transient [42] (see [39] for a discussion of its detectability). Knowing the environment around the merger is pivotal since the initial conditions that should be used in the numerical simulations depend on this information.

5 Conclusions

Since the 1960's, considerable progress has been made in the numerical community. The successful simulations of BBH coalescence in 2005 have been a watershed in the history of NR. The concepts of 3+1 space-time split, the ADM equations, and the BSSN formulation all played important roles in the development of NR leading to the moving puncture breakthrough and continue to be used today. The gravitational waveforms predicted from the numerics was observed experimentally in 2015, which established the validity of GR in the strong-field regime.

References

[1] G. Darmois, "Les équations de la gravitation einsteinienne," *Meml. des Sci. Math.*, vol. 25, 1927.

[2] A. Lichnerowicz, "Sur certains problèmes globaux relatifs au système des équations d'Einstein," *Actual. Sci. Ind.*, vol. 833, 1939.

[3] A. Lichnerowicz, "L'integration des équations de la gravitation relativiste et le problème des n corps," *J. Math. Pures Appl.*, vol. 23, no. 37, 1944.

[4] A. Lichnerowicz, "Sur les équations relativistes de la gravitation," *Bull. la S.M.F.*, vol. 80, no. 237, 1952.

[5] Y. Choquet-Bruhat, "Théorème d'existence pour certains systèms d'équations aux dérivées partielles non linéaires," *Acta Math.*, vol. 88, no. 141, 1952.

[6] Y. Choquet-Bruhat, "Sur l'Intégration des Équations de la Relativité Gérale," *J. Ration. Mech. Anal.*, vol. 5, no. 951, 1956.

[7] P. A. M. Dirac, "The Theory of Gravitation in Hamiltonian Form," *Proc. R. Soc. London A Math. Phys. Eng. Sci.*, vol. 246, no. 1246, pp. 333–343, 1958.

[8] P. A. M. Dirac, "Fixation of coordinates in the Hamiltonian theory of gravitation," *Phys. Rev.*, vol. 114, no. 3, pp. 924–930, 1959.

[9] R. Arnowitt, S. Deser, and C. W. Misner, "The Dynamics of General Relativity," *Gen. Relativ. Gravit.*, vol. 40, no. 9, pp. 1997–2027, 2004.

[10] T. W. BAUMGARTE, *Numerical Relativity: Solving Einstein's Equations on the Computer*. Cambridge University Press, 2010.

[11] J. W. York Jr, "Kinematics and dynamics of general relativity," *Sources gravitational radiation; Proc. Work.*, pp. 83–126, 1979.

[12] J. W. York Jr and T. Piran, "The initial value problem and beyond," *Spacetime Geom.*, vol. 1, 1982.

[13] E. Gourgoulhon, "3+1 Formalism and Bases of Numerical Relativity," *arXiv: gr-qc/0703035*, no. March, p. 220, 2007.

[14] M. ALCUBIERRE, *Introduction to 3+1 Numerical Relativity*. Oxford University Press, 2008.

[15] U. Sperhake, "The numerical relativity breakthrough for binary black holes," *Class. Quantum Gravity*, vol. 32, no. 12, p. 124011, 2015.

[16] T. Nakamura, K. Oohara, and Y. Kojima, "General relativistic collapse to black holes and gravitational waves from black holes," *Prog. Theor. Phys. Suppl.*, vol. 90, 1987.

[17] L. E. Kidder, M. A. Scheel, and S. A. Teukolsky, "Extending the lifetime of 3D black hole computations with a new hyperbolic system of evolution equations," *Phys. Rev. D*, vol. 64, no. 6, pp. 1–13, 2001.

[18] M. Shibata, "Status of numerical relativity," *Pramana - J. Phys.*, vol. 63, no. 4, pp. 703–715, 2004.

[19] M. Shibata and T. Nakamura, "Evolution of three-dimensional gravitational waves: Harmonic slicing case," *Phys. Rev. D*, vol. 52, no. 10, pp. 5428–5444, 1995.

[20] M. Shibata, K. Taniguchi, and K. Uryu, "Merger of binary neutron stars of unequal mass in full general relativity," *Phys. Rev. D*, vol. 68, no. 8, pp. 1–24, 2003.

[21] T. W. Baumgarte and S. L. Shapiro, "Numerical integration of Einstein's field equations," *Phys. Rev. D*, vol. 59, no. 2, p. 024007, 1998.

[22] H. J. Yo, T. W. Baumgarte, and S. L. Shapiro, "A numerical testbed for singularity excision in moving black hole spacetimes," *Numer. Algorithms*, vol. 64, p. 13, 2001.

[23] H.-J. Yo, T. W. Baumgarte, and S. L. Shapiro, "Improved numerical stability of stationary black hole evolution calculations," *Phys. Rev. D*, p. 13, 2002.

[24] M. Alcubierre, G. Allen, B. Bruegmann, E. Seidel, and W.-m. Suen, "Towards an understanding of the stability properties of the 3+1 evolution equations in general relativity," *Phys. Rev. D*, vol. 62, p. 15, 2000.

[25] M. Alcubierre, B. Brügmann, D. Pollney, E. Seidel, and R. Takahashi, "Black hole excision for dynamic black holes," *Phys. Rev. D*, vol. 64, no. 6, pp. 1–5, 2001.

[26] M. Campanelli, C. O. Lousto, P. Marronetti, and Y. Zlochower, "Accurate evolutions of orbiting black-hole binaries without excision," *Phys. Rev. Lett.*, vol. 96, no. 11, 2006.

[27] J. G. Baker, J. M. Centrella, D.-I. Choi, M. Koppitz, and J. R. van Meter, "Gravitational-wave extraction from an inspiraling configuration of merging black holes," *Phys. Rev. Lett.*, vol. 96, no. 11, 2006.

[28] J. Thornburg, *Numerical relativity in black hole spacetimes*. PhD thesis, The University of British Columbia, 1993.

[29] A. Einstein and N. Rosen, "The particle problem in the general theory of relativity," *Phys. Rev.*, vol. 48, no. 1, pp. 73–77, 1935.

[30] D. R. Brill and R. W. Lindquist, "Interaction energy in geometrostatics," *Phys. Rev.*, vol. 131, no. 1, pp. 471–476, 1963.

[31] J. M. Centrella, J. G. Baker, B. J. Kelly, and J. R. van Meter, "Black-hole binaries, gravitational waves, and numerical relativity," *Rev. Mod. Phys.*, vol. 82, no. 4, pp. 3069–3119, 2010.

[32] M. Shibata, *Numerical Relativity: 100 Years of General Relativity, vol. 1*. World Scientific, 2016.

[33] M. Boyle, D. A. Brown, L. E. Kidder, A. H. Mroué, H. P. Pfeiffer, M. A. Scheel, G. B. Cook, and S. A. Teukolsky, "High-accuracy comparison of numerical relativity simulations with post-Newtonian expansions," *Phys. Rev. D - Part. Fields, Gravit. Cosmol.*, vol. 76, no. 12, pp. 1–31, 2007.

[34] M. Hobson, G. Efstathiou, and A. Lasenby, *General Relativity: An Introduction for Physicists*. Cambridge University Press, 2006.

[35] É. E. Flanagan and S. A. Hughes, "The basics of gravitational wave theory," *New J. Phys.*, vol. 7, no. 1, p. 204, 2005.

[36] M. A. Scheel, M. Boyle, T. Chu, L. E. Kidder, K. D. Matthews, and H. P. Pfeiffer, "High-accuracy waveforms for binary black hole inspiral, merger, and ringdown," *Phys. Rev. D - Part. Fields, Gravit. Cosmol.*, vol. 79, no. 2, pp. 1–14, 2009.

[37] Abbott and Others, "Observation of gravitational waves from a binary black hole merger," *Phys. Rev. Lett.*, vol. 116, no. 6, p. 61102, 2016.

[38] K. Belczynski, S. Repetto, D. E. Holz, R. O'Shaughnessy, T. Bulik, E. Berti, C. Fryer, and M. Dominik, "Compact Binary Merger Rates: Comparison With Ligo/Virgo Upper Limits," *Astrophys. J.*, vol. 819, no. 2, p. 108, 2016.

[39] S. Rosswog and Others, "Detectability of compact binary merger macronovae," *Class. Quantum Gravity*, vol. 34, no. 10, 2017.

[40] C. Freiburghaus, S. Rosswog, and F.-K. Thielemann, "R-Process in Neutron Star Mergers," *Astrophys. J.*, vol. 525, no. 2, pp. 121–124, 1999.

[41] J. M. Lattimer and D. N. Schramm, "The tidal disruption of neutron stars by black holes in close binaries," *Astrophys. J.*, vol. 210, p. 549, 1976.

[42] L. F. Roberts, D. Kasen, W. H. Lee, and E. Ramirez-Ruiz, "Electromagnetic Transients Powered By Nuclear Decay in the Tidal Tails of Coalescing Compact Binaries," *Astrophys. J.*, vol. 736, no. 1, p. L21, 2011.